Light Metals 2012 *Edited by: Carlos E. Suarez*
TMS (The Minerals, Metals & Materials Society), 2012

ELECTROHYDRAULIC SHEET METAL FORMING OF ALUMINUM PANELS

John J.F. Bonnen[1], Sergey F. Golovashchenko[1], Scott A. Dawson[1], Alexander V. Mamutov[2], Alan J. Gillard[1]
[1]Ford Research and Advanced Engineering, Dearborn, Michigan / USA;
[2]Department of Mechanical Engineering, Oakland University, Rochester, Michigan / USA

Keywords: Aluminum, Hydroforming, Electro-hydraulic Forming, Pulsed Forming

Abstract

In this paper, we present results of testing from sheet metal forming trials using pulsed electrohydraulic technology. Pulsed electrohydraulic forming is an electrodynamic process, based upon high-voltage discharge of capacitors between two electrodes positioned in a fluid-filled chamber. Electrohydraulic forming (EHF) combines the advantages of both high-rate deformation and conventional hydroforming; EHF enables a more uniform distribution of strains, widens the formability window, and reduces elastic springback in the final part when compared to traditional sheet metal stamping. This extended formability allows the fabrication of aluminum panels that are difficult to make conventionally even of EDDQ steel, and it thereby vastly improves the number automotive weight reduction opportunities. The paper presents discoveries regarding chamber design, electrode erosion, forming, and results of finite element multiphysics simulations of system performance.

Introduction

As energy costs and regulatory pressures increase on the automotive industry, aluminum alloys (AA) are being increasingly used to achieve lightweight automotive body construction. Unfortunately, formability levels offered by aluminums do not match those of mild and bake hardenable steels and thus further development of sheet metal forming technologies is necessary to broaden the application of aluminums in the automotive industry. Hydromechanical drawing (hydroforming) offers deeper drawing and more uniform distribution of strains due to substantial frictional reductions. An increase in either the maximum achievable strain which a material can withstand without fracture or a significant reduction in springback would further promote application of aluminum ground vehicles. EHF, a form of pulsed forming, is capable of achieving such improvements. In EHF a significant amount of stored electrical energy is discharged across an electrode gap in a water-filled chamber. The brief, intense discharge (< 100 microseconds) causes a plasma channel to form between the electrodes which subsequently vaporizes a small volume of liquid. Channel formation and water vaporization cause a high intensity/high velocity shock wave to propagate through the liquid. The shock wave propagates toward a sheet metal blank driving it into a die clamped to the chamber. Since the liquid transmits the force, only a die (no punch) is required. Compared to electromagnetic forming (EMF) processes, EHF is applicable to wider variety of sheet metals without any special conductivity constraints. EHF requires a single tool as multiple pulses may be used to form the part. In EMF several different sets of coils and dies are often necessary[1].

History

Initial development of EHF technology began in Russia in the early 1950's by Yutkin [2]. Bruno [3], and Davies and Austin [4] reviewed early applications and research results on EHF. In early development most of the effort was dedicated to form low volume parts at low cost. A significant advantage of EHF compared to traditional sheet metal forming technology is that it does not require two matching dies: a punch is usually replaced by liquid, transmitting pressure from the discharge channel to the surface of the blank. Bruno [3] described a number of industrial examples where EHF machines storing anywhere from 36kJ to 172kJ were employed. However, due to the necessity to fill the chamber with liquid at the beginning of each forming cycle and evacuate it at the end, cycle times for EHF have traditionally been in the range of several minutes. Sanford [5] described a hybrid technology where static hydroforming was used to initially bulge sheet metal into the die cavity, and this step was followed by EHF which, through higher pressure levels, filled the details of the die cavity but with a cycle time of 10 minutes.

More recently, Balanethiram and Daehn [6] reported increased forming limits compared to conventional techniques when EHF forming into a conical die: the maximum strain for plane strain conditions was increased by a factor of 2.5 for copper and by a factor of 5 for AA6061-T4.

Very limited attempts have been made to simulate the EHF process. Golovashchenko and Mamutov [7] presented results of bulging into an open round die. Vohnut et al [8] reported results of pulsed loading in a closed volume, assuming energy equivalence to explosive forming.

The project objective is to develop EHF technology to the point where it is suitable for high volume production, enabling critical weight savings and improving fuel economy for cars and trucks. Critical to the implementation of this technology is the need to establish the benefits of EHF, to demonstrate the ability to reliably and robustly create discharges in the chamber, to form otherwise unformable parts with reduced springback and lastly to establish the necessary predictive tools to properly design parts and tooling.

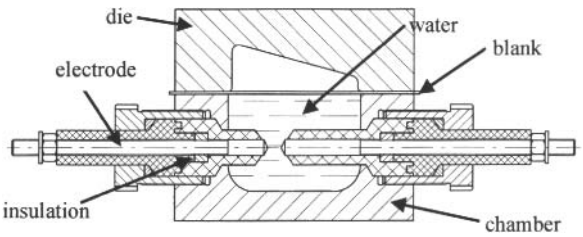

Figure 1. Design of the electrohydraulic forming tool: side cross-section of the chamber.

Experimental Setup

A schematic illustration of an EHF system is shown in Figure 1. The water-filled chamber at bottom has a pair of electrodes inserted into the chamber cavity. On top of the chamber rests a sheet metal blank, and on top of that rests the female die with the desired part shape. In order to control material flow into the die,

the tool often includes a binder used to help locate the blank in the tool. A critical part of the tool design is the seals between the chamber/binder and blank which are required to keep the liquid within the chamber. Another set of seals is located between the die and the blank – necessary to allow evacuation of the space between the die and blank. The entire assembly is clamped in a press.

A pulsed current generator is attached to the electrodes and the chamber itself is connected to a system that provides water, air pressure and vacuum. Optionally, a static hydroforming unit is attached to preform the blank in-situ. A hydraulic press is used to clamp the tool in place and an automation unit is used to deliver blanks into the tool and remove parts after forming.

Before the cycle is started the liquid is brought to a level just below the chamber top to minimize both the likelihood of spillage and the liquid volume which is moved in and out of the EHF chamber. The automation then places a blank on the chamber and press closes and clamps the die and chamber together. Water fills the chamber and vents are provided near the parting line to help minimize air within the system. A vacuum is placed on the vent holes in order to assist the chamber filling operation and minimize air pockets – air in the system is a source of considerable loss of efficiency. The cavity between the die and blank is then evacuated since air here acts as a barrier to final corner filling operations.

At this point the water pressure in the chamber may be increased to an extent sufficient to deform the blank partially into the die cavity. This pre-forming operation reduces the overall number of discharges necessary to fully form the part and potentially reduces overall cycle time, but the pressure must be relieved because excess water pressure suppresses plasma channel formation [9].

The deformation process begins once the output of the pulse generator (5-15kV) is placed on the electrodes. The voltage sits on the electrodes while a lightning-like conduction channel develops between the electrode tips. Once formed, current begins to flow and a plasma rapidly develops between the tips. The plasma is a very low conductivity ionized gaseous channel connecting the electrodes that conduct large currents (50-100kA). The high energy density causes the plasma to rapidly expand and converting liquid water to high pressure steam and causing a shockwave to propagate into the liquid and away from the electrodes.

The shockwave drives the water into the blank and the blank accelerates toward the die surface. Since large blank velocities can cause the blank to rebound off of the die surface with resulting die damage and possible rupture of the blank, multiple discharges are typically used to form the part to approach the die surface incrementally. Once the blank has deflected, water is allowed to refill the chamber. The back-fill of the chamber with water after each pulse eliminates this extra volume occupied by a pocket of low pressure air and water vapour that would be compressed/heated with each subsequent pulse, substantially reducing subsequent shock waves delivered to the blank. This incremental volume of water is carefully measured in order to monitor part deformation.

Subsequent pulses/discharges require monotonically increasing energy levels, and the energy/pressure of each forming pulse is controlled by adjusting the maximum charging voltage applied to the capacitors. The final energy level is normally dictated by the part details (corner filling operations require the highest energy levels/pressures), the shape of the chamber and the blank material.

The injected volume of water decreases with each subsequent pulse decreasing to zero when the part is fully formed. The totalized volume of water used to fill the chamber between discharges is used to determine whether the part has been fully formed. Once formed water is drained back down to the initial level, the press opened, and the part removed.

Electrode System

Of the major components, the electrodes are the heart of the system and must endure the harshest environment. They must deliver 100kA safely into and out of the chamber, insulate the chamber from potentials up to 15kV, and withstand the high energy densities, temperatures and pressures generated by the discharge. They must maintain a water tight seal, be adjustable so that the inter-electrode gap may be set, and they must resist the forces resulting from large pressures that tend to eject them from the chamber. Lastly, they must be able to withstand the erosion caused by the electrical discharge and the high pressures generated in the chamber.

A program was begun to identify the basic electrode material and tip geometry. A number of electrodes with different tip shapes and materials were tested in the experimental chamber (Figure 2). The volume of the liquid in the chamber was quite small, a fraction of the volume of a chamber which can accommodate an automotive panel. A thick steel plate was used in place of the sheet metal blank and die to seal the chamber. This smaller, much more highly constrained, volume significantly increases pressures and accelerates the durability component of the test. Up to 120 11kV (12.1kJ) pulses were discharged through each pair of electrodes, and periodically the chamber was opened and the electrodes were inspected for damage. At the end of the test the total electrode erosion was documented.

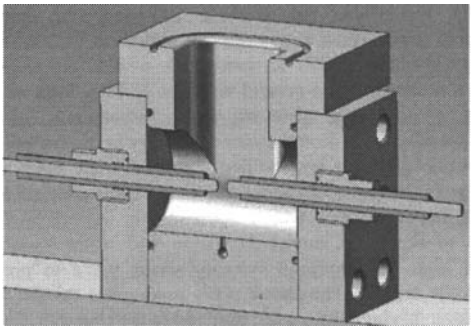

Figure 2. 1.8 liter electrode testing chamber. A thick steel plate covers the top during testing.

Electrode tests were conducted on steel, molybdenum, tungsten, and a copper-tungsten powder metallurgy alloy. The electrodes were constructed with hemispherical tips and tested in the chamber for up to 120 discharges. Of these materials, only the steel survived the full 120 discharges. Molybdenum survived 15 discharges before the electrode fractured outside the chamber at the pulse generator attachment point. The electrode broke two more times in a similar fashion and the test was suspended. The tungsten broke in a similar fashion after a single discharge. The tungsten-copper PM material broke inside the chamber due to the

bending forces after roughly 70 discharges. Volumetric erosion measurements were conducted on the first three materials, shown in Figure 3, and indicate that, as expected, the molybdenum showed better erosion performance – the tungsten did not have enough discharges on it to be measured. Unfortunately, the prohibitive material and machining costs associated with these refractory metals and their poor (non-erosion) performance makes steel the clear choice.

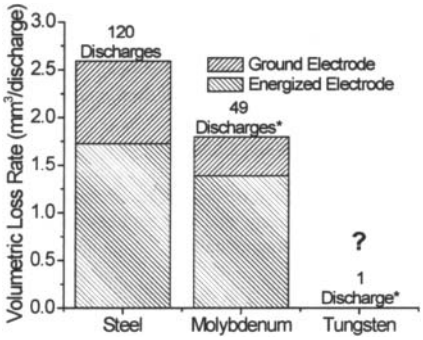

Figure 3. Volumetric erosion rate per discharge for electrode materials. Tungsten erosion could not be measured.

Electrode insulation materials were tested as well. Plastics with good insulation performance must be machined rather than cast in place, and these materials were tested with a special split-insulation electrode design and pulsed until failure. The results, found in Table 1, include the number of pulses until failure, the failure mechanism (mechanical or electrical) and the failure location. The best performing materials failed mechanically near the electrode tip and the worst failed at the chamber entry point. Generally when the failure was at the chamber entry it was via an electrical pulse that punched through the insulation and eventually caused a mechanical failure. Tip failures were uniformly mechanical damage via pulsed pressure. The best two insulation materials turned out to be ultra high molecular weight polyethylene and polyurethane. The difference in life was sufficiently small that polyurethane was chosen because it is easily cast into form.

Table 1. Insulation Material Performance

Insulation Type	Failure Pulses	Failure Loc./Type
Ultra High Molecular Weight Polyethylene (UHMW PE)	700	Tip/Mechanical
Polyurethane	650	Tip/Mechanical
Acetyl	180	Chamb.Entry / Elect.
Polycarbonate	120	Chamb.Entry / Elect
Polysulfone	46	Chamb.Entry / Elect

Another series of tests was conducted to determine optimum tip shape. The electrode profile or tip shape can significantly influence the electrostatic fields set up after the voltage is applied to the electrodes and affects plasma channel formation and timing. The inter-electrode gap has even more influence on these processes. While the electrical performance was closely studied it turned out that tip erosion rates and consequent inter-electrode gap increase was the real driver. In order of greatest electrical efficiency to least, the shapes studied were: conical, hemispherical, and cylindrical (or flat). Figure 4 shows a bar chart indicating the linear electrode length loss and volumetric loss.

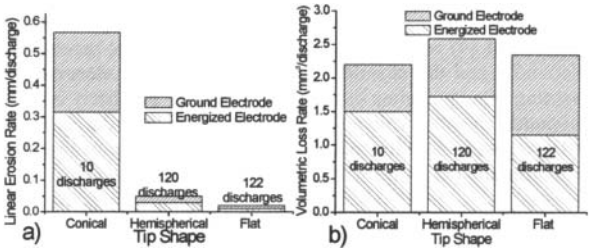

Figure 4. Linear and volumetric erosion rates of steel electrodes with different initial tip shapes.

Figure 5. Stable as-eroded electrode tips showing similar profiles.

In Figure 4a the linear erosion rate per discharge was so severe for the conical tipped electrodes that the test was suspended after ten discharges because of significant gap increase and subsequent electrical instability. The hemispherical tip electrodes fared much better and exhibited a substantially lower linear erosion rate. The flat tipped electrodes had half again the erosion rate of the hemispherical. The reason for this performance becomes clear in Figure 4b. Regardless of the tip shape, the volumetric erosion rate is constant. The erosion rate of the energized electrode is about 40% higher than that of the ground electrode.

A large number of experiments were run on electrode pairs with different tip shapes, and sufficient pulses were placed on them until the original tip was worn away. It was noted that they all attained a similar, stable, as-eroded tip profile, as seen in Figure 5. From an electrode gap point of view, this profile is clearly the most stable and leads to the lowest linear erosion rate.

Each tip profile was digitized and analyzed, and it was found that the best fit function was a modified Arrhenius of the form $y(x) = y_o - A_1 e^{-(1-x)/t_1} - A_2 e^{-(1-x)/t_2} - A_3 e^{-(1-x)/t_3}$, where y is the electrode height measured from the tip, $x = r / R_o$, the ratio of the distance from the electrode centerline divided by the electrode radius R_o, [10]. The average profile may be described as: $y_o = 0.00365$; $A_1 = 0.598$; $t_1 = 0.199$; $A_2 = 0.713$; $t_2 = 0.0126$; $A_3 = 0.197$; $t_3 = 0.00065$. The advantage of this profile is that it is stable, has predictable electrical performance and minimizes the necessary linear advancement of the electrode to correct for erosion.

Periodically the electrodes are advanced towards each other to compensate for tip erosion. Analysis of pulse data indicate that, as the inter-electrode gap increases, there is a slight decrease in the amplitude of the pressure pulse. However, this decrease is compensated by a slight increase in the duration of the pressure pulse. In general, the process is robust and not sensitive to the changes in clearance between the electrodes.

Chamber Design

Chamber durability is a key concern in production. As a chamber must essentially contain an explosion, the chambers used in EHF

tend to be very thick walled pressure vessels. Experience based guidelines have been developed over time. The guidelines that improve durability/safety are: (1) thick walls, (2) constructed from tough steel, (3) minimize the places where air pockets may get trapped, (4) where possible maximize the distance between the electrodes and the chamber wall, and (5) support electrodes in bending. One guideline that improves forming efficiency is to (6) minimize chamber volume as much as possible. An early 1.3 liter version of the electrode testing chamber, shown in Figure 6, demonstrated the problem with guidelines (2), (3) and (4).

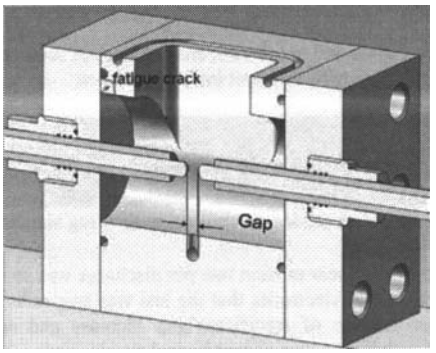

Figure 6. 1.3 liter electrode testing chamber.

Although over 30mm thick and supported by the clamping press, the archway over the electrodes broke after roughly 2000 pulses as marked in the figure. Entrained air caught under the arch helped caused cavitation at the top of the arch which cut a notch that subsequently led to a fatigue failure. Other than the water leak there was no cataclysmic failure because the chamber was constructed of lower hardness/tough steel. Finite element analysis of the newer chamber design (Figure 2) indicated that the stresses were much improved – cavitation damage was discovered in the side walls after this second chamber was constructed and used in electrode testing.

Development of a chamber for a production part followed along the same general principals. The initial version of the production chamber and binder ring, shown in Figure 7a has electrodes at a right angle to the chamber wall. In this design discharges caused bending in the electrodes and subsequent fatigue cracking. In the redesigned chamber the electrodes are directly opposed, the binder is integrated and chamber was volume minimized and shape optimized with the tools discussed in the Forming Simulation section.

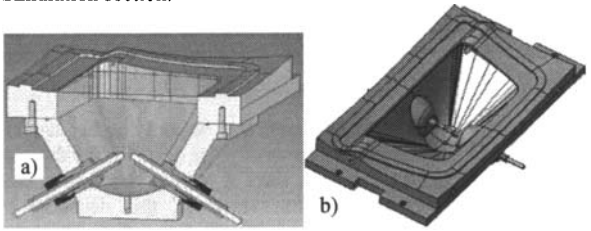

Figure 7. a) initial chamber design and b) final chamber design.

Forming Simulation

Modelling the EHF process is a considerable challenge because of the multiphysics nature of the process. Consider that first electrical energy must be converted into plasma. There is a boundary between the high pressure plasma and high pressure water vapor, and a further boundary between the water vapour and the (compressible) liquid. The liquid interfaces with the steel blank, and the steel blank accelerates and at some point must interact with the die surface. Models must be developed for: 1) the electrical nature of the discharge channel; 2) physical plasma/water vapor channel; 3) the liquid as a pressure transmitting media; 4) blank deformation; 5) chamber deformation and 6) the blank in contact with the die. These models must be coupled, and the boundaries between phases must be permitted to translate. Lastly, there is the challenge of developing a correct contact model between blank and die. The individual models were developed and then coupled in LS DYNA.

Electrical Discharge Channel Model

The differential equation for current $i(t)$ in the circuit in Figure 8 includes variable resistance of discharge channel, R_v, cumulative resistance of pulsed forming machine and connecting cables, R_0, and inductance of discharge circuit L.

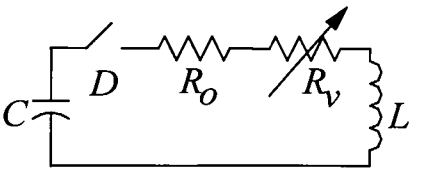

Fig. 8 High-voltage discharge circuit (C = 50 μF – pulse generator capacitance [initial charge, U_o=12.5 kV], L – total system inductance, R_o – resistance of the circuit external to the discharge channel, R_v – resistance of the discharge channel)

The differential equation for current $i(t)$ in the circuit of Fig. 8 includes variable resistance of discharge channel, R_v, cumulative resistance of pulsed forming machine and connecting cables, R_0, and total inductance of discharge circuit L . It can be written in the following form,

$$\frac{d^2 i}{dt^2} + \frac{R_v(i,t) + R_0}{L} \cdot \frac{di}{dt} + \frac{1}{LC} i = 0 \quad , \tag{1}$$

and has the following initial conditions

$$i(0) = 0, \qquad \left.\frac{di}{dt}\right|_{t=0} = -\frac{U_0}{L} \quad , \tag{2}$$

where U_0 = 12.5kV, the initial voltage of capacitor. The electric power being driven through the discharge channel is defined by:

$$N = i^2 R_v(i,t) \quad . \tag{3}$$

Integration of equation (3) over time allows one to determine the energy uniformly deposited throughout the discharge channel,

$$E_{ch}(t) = \int_0^t i^2(t) R_v(i,t) dt \cdot \tag{4}$$

The plasma channel is modelled in LS DYNA as an adiabatically expanding gas. The plasma channel pressure is calculated as $p_{ch} = (\gamma - 1)(\rho/\rho_0)E$ where γ is the adiabatic coefficient for plasma produced from tap water, and where ρ_0 is the initial mass density,

ρ is the instantaneous mass density, and E is the fraction of the energy.

Liquid Phase Model

The liquid was modelled in LS DYNA as an ideal compressible liquid with a specific cavitation threshold. Required parameters are the initial mass density, compression modulus and negative pressure threshold corresponding to initial cavitation. Heat transfer between the plasma and liquid is not currently modelled.

Experimental validation

Initial experimental validation of the discharge channel and pressure transmission models in a water filled chamber was conducted in a very simple configuration consisting of a tubular chamber with a discharge on the symmetry line. The pressure was measured by a calibrated piezoelectric gauge mounted inside the wall of the chamber. The process was simulated in a one-dimensional formulation assuming that the walls of the chamber are rigid and neglecting the edges of the cylindrical chamber. More detail of the experimental validation may be found in [11].The model was initialized with the capacitance and a 12.5 kV initial voltage but the resistance and inductance were not directly input into the model. Instead, the experimental data energy curve was input into the model.

Sheet Metal Blank Model

Two different approaches were employed in this project to model the deformation of the sheet metal blank into its final shape: 1) a model constructed of elastic-plastic shell elements incorporating bending stiffness and in contact with the rigid die can efficiently predict strain distributions and potential fracture in the blank; 2) elastic-plastic solid elements in contact with a deformable die will predict die loads and provides more accuracy in sharp corner filling operations. The elevated strain rate material behaviour is modelled in a fashion similar to that of quasi static forming processes.

Process Modelling

A full simulation of the EHF production process was performed for the license plate pocket. As mentioned earlier, actual part formation requires several pulses. The blank deformation analysis correctly indicated that the largest total strains occur during the final forming step. The highest pressures are required in this last forming step in order to fill sharp corners. The shape of the optimized chamber design is shown in Figure 7b and the one-sided die geometry is shown in Figure 9.

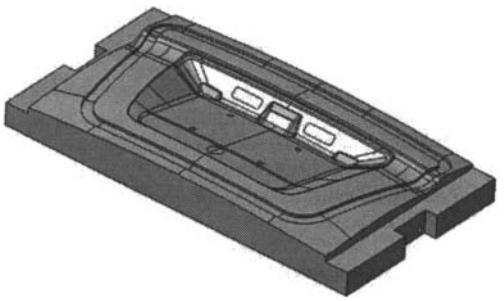

Figure 9. Geometry of the die. Chamber is shown in Figure 7b.

Simulation of the first stage, binder closing, was made using a conventional explicit mechanical LS-DYNA solver. It finished in about one hour. The following stages include simulation of the expansion of an initially very small gas/plasma bubble in water. This very small initial volume requires a very fine numerical mesh within the bubble, which dictated a very small time integration step and, therefore, required a substantial increase in calculation time.

The evolution of both the discharge channel shape and the blank deformation during the first EHF discharge are shown in Figure 10. The initial conditions shown in the 0.033ms step represents the output of the 2D simulation. It is necessary to use a relatively low energy level in the first discharge to avoid possible rebound of the blank off of the die surface. Therefore, the shape of the blank after the first discharge is fairly smooth with generous corner radii.

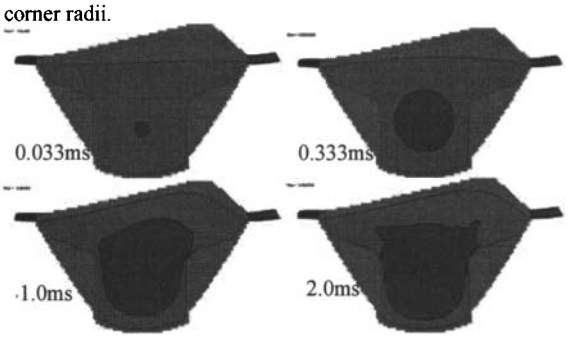

Figure 10. Channel expansion and deformation of the blank during the first EHF discharge.

The progress of blank deformation after each discharge is shown in Figure 11. The distribution of plastic deformation after each discharge is shown in Figure 12. Note that after the third discharge the amount of strain localization almost doubles. Before the last step (third EHF step), it was necessary to refine the blank's mesh for a more accurate representation of critical sharp corners. The model complexity prevented the use of automatic adaptive remeshing.

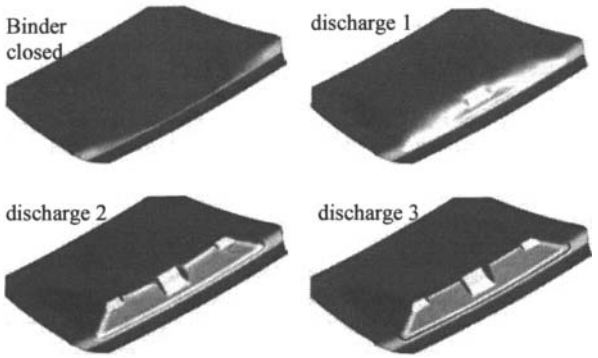

Figure 11. Changing blank geometry

Instead, an additional intermediate calculation was made with an adaptive refinement step. It was performed on a simplified model without the ALE portions of the mesh, and it was performed with no loads or tool deflections applied. The simulation was initiated, adaptive refinement allowed to occur, and a single integration step was calculated – in a few minutes at most. The refined blank mesh was then transferred back into the simulation for the last discharge.

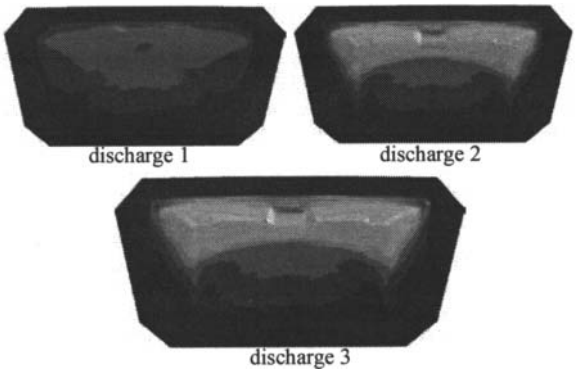

Figure 12. Distribution of plastic strains within the blank after each EHF discharge.

The average element size in the mesh was refined down to 1 mm from 2 mm – an acceptable level for accurate representation of critical geometries. However, this refinement introduced numerical defects when it was run against the liquid's relatively coarse 3 mm ALE mesh and affected the maximum deformation value at critical points. Thus, a reduction in the ALE element size was required and resulted in about three times the number of elements for the same volume, (up to approximately 2 million). Simulation time increased to 8 hours for the third stage. Although a smaller ALE element size was desirable, further refinement of the ALE mesh was impossible because of the unrealistic increase in simulation time required.

Discussion

The EHF process is fairly complex. Designing tooling to work in this extreme environment is challenging. It is believed that the pressures in the neighborhood of the electrodes can reach as high as 2GPa [12] and these pressures can cause significant damage to the chamber, seals, and electrode system if the systems are not designed properly. Significant effort has gone into understanding the electrode system and how to manage durability. Long term electrode tests are planned to understand and manage the durability of the electrodes for production usage – it is important that they last at least one shift.

Results of numerical simulations to date have, with fair effort, matched reasonably well with the modicum of experimental data that we have been able to extract directly from the harsh environment inside the chamber. The modeling illustrates the complex mechanisms within the EHF process.

Conclusions

As a result of the recent developmental work on EHF technology reported in this paper, important enablers have been developed towards making EHF stamping possible: (1) extension of the electrode life and minimizing of the electrode system maintenance based on electrode erosion studies which indicated that steel electrodes with a modified Arrhenius shape were optimal, and, further, polyurethane was found to be the optimal insulator for in-chamber usage; (2) durable and safe chamber designs are now constructed with newly developed EHF process simulation tools, and (3) EHF numerical process simulation tools have been developed to the point where they are now sufficient to the task of tooling development and optimization of both the chamber shape, electrode position and deformation modelling.

Acknowledgement

This material is based upon work supported by the Industrial Technology Program of the US Department of Energy under Award Number DE-FG36-08GO18128.

References

1. S.F. Golovashchenko, "Material Formability and Coil Design in Electromagnetic Forming," *Journal of Materials Engineering and Performance*, 16 (3) (2007), 314-320.
2. L.A. Yutkin, "Electrohydraulic Effect", *Mashgiz* (in Russian). (Moscow, Russia 1955)
3. E.J. Bruno, *High-Velocity Forming Of Metals.* (Dearborn, MI, USA, American Society of Tool and Manufacturing Engineers, 1968).
4. R. Davies and E.R. Austin, *Development In High Speed Metal Forming*, (New York, USA., Industrial Press Inc. 1970)
5. J.E. Sandford, "High Velocity Takes Off Again," *Iron Age* (3) (1969) 91-95.
6. V.S. Balanethiram, and G.S. Daehn, "Hyperplasticity: increased forming limits at high workpiece velocity". *Scripta Metallurgica et Materialia*, 30 (1994), 515-520.
7. S.F. Golovashchenko and V.S. Mamutov. "Electrohydraulic Forming of Automotive Panels," (In: Proc. of 6th Global Innovations Symposium: Trends in Materials and Manufacturing Technologies for Transportation Industries, TMS, San Francisco, CA, USA, February 13-17, 2005), 65-70.
8. V.J. Vohnout, G. Fenton and G.S. Daehn, "Pressure Heterogenity in Small Displacement Electrohydraulic Forming Process,". (In: Proc. of 4th International Conference on High Speed Forming, Columbus, OH, USA, March 9-10, 2010) 65-74.
9. S.F. Golovashchenko, A.J. Gillard, D. Piccard and A.M. Ilinich, "Electrohydraulic Forming Tool and Method of Forming Sheet Metal Blank with the Same," US Patent 7,802,457 (28 September 2010).
10. J.J.F. Bonnen, S.F. Golovashchenko and S.A. Dawson, "Electrode Assembly For Electrohydraulic Forming Process", US Patent Application 12/940,235. (5 November 2010)
11. S.F. Golovashchenko, A.V. Mamutov, J.J.F. Bonnen and A.J. Gillard, "Electrohydraulic Forming of Sheet Metal Parts," (In Proc. ICTP, Germany, 2011) 1170-1175.
12. V.N.Chachin, *Electrohydraulic treatment of materials* (Minsk: Science and Engineering, 1978), 183